DNA Nanofibers

DOI: 10.1002/anie.200900885

White Luminescence from Multiple-Dye-Doped Electrospun DNA Nanofibers by Fluorescence Resonance Energy Transfer**

*Yogesh Ner, James G. Grote, Jeffrey A. Stuart, and Gregory A. Sotzing**

The natural process of photosynthesis provides an efficient example of the hierarchical organization of molecules for energy transfer. Self-assembly of biomolecules provides an opportunity to mimic such orderliness to design efficient optoelectronic materials. Herein, we demonstrate the fabrication of white-luminescent DNA-based nanofibers through the self-organization of a DNA–lipid complex and fluorescence resonance energy transfer (FRET)-based simultaneous light emission. Coumarin 102 (Cm102) and 4-[4-dimethylaminostyryl]-1-docosylpyridinium bromide (Hemi22) were used as donor and acceptor, respectively, which associate with DNA through different mechanisms. The result is a distribution of immobilized dye molecules with an optimized spatial organization that favors efficient energy transfer, even at low acceptor-loading levels. The emission wavelength is controlled by varying the donor-to-acceptor ratio, which shifts the fluorescence from blue to orange through pure white. In the resulting synergistic system, DNA facilitates emission of white light by imposing both spatial organization and specific binding environments for the dye molecules, while the emission intensity is enhanced by the geometry of the electrospun fiber.

The merging of optoelectronics, photonics, and nanoscience could lead to optimized materials for electromagnetic energy manipulation. Regulation of nonradiative energy transfer (e.g., FRET) provides an important route toward improving device performance.[1] However, obtaining the appropriate spatial organization for efficient energy transfer is a key challenge; a structural matrix is required that furnishes both orientation and proximity between donor and acceptor molecules. Without such an arrangement, fine control of energy transfer is not possible; at low dye concentrations FRET will occur either with poor efficiency or not at all, and at higher concentrations the signal will be dominated by the acceptor, or quenched as a result of aggregation. Nanoarchitectures can act as platforms for efficient energy transfer by providing an optimized spatial distribution. Various nanostructures have been used for controlled energy transfer, including silica nanoparticles,[2] polymer–mesoporous silica composites,[3] thin films of diblock-copolymer micelles,[4] dendrimers,[5] and self-assembled fibers.[6]

DNA complexed with a cationic surfactant has emerged as an intriguing candidate for optoelectronic applications because of its unique material properties, including solubility in organic solvents and ability to form thermally stable, transparent films.[7,8] These novel materials have potential for optical memory matrices, field-effect transistors, photochromic switches, electrooptic waveguides, and as electron-blocking layers for light-emitting diodes (LEDs).[9,10] Amplified spontaneous emission has been observed when these materials are used as a matrix for laser dyes.[11] We have demonstrated that DNA complexed with cationic surfactants can readily be electrospun into nanofibers.[12] Incorporation of a hemicyanine fluorophore produced nanofibers with enhanced fluorescence yield, as a result of both fiber geometry and interactions between the dye and DNA. The intrinsic lattice structure within these fibers organizes and isolates individual dye molecules, thereby minimizing aggregation-induced quenching. Herein, we report the generation of FRET-based white luminescence in electrospun DNA-based nanofibers doped with multiple fluorophores.

Nanofibers of salmon DNA complexed with the cationic lipid surfactant cetyltrimethylammonium chloride (CTMA) were produced by electrospinning. The field-emission scanning electron microscopy (FESEM) image of electrospun fibers of DNA–CTMA is shown in Figure 1a. The average fiber diameter was found to be 300 nm. DNA–CTMA complexes are known to form ordered, mesophasic film morphologies; coordination between the DNA phosphate and the CTMA ammonium groups results in lamellar structures of aligned, parallel DNA, sandwiched by CTMA layers.[7,8,13] In thin films of DNA–CTMA, X-ray diffraction revealed structural anisotropy between the side edge and the film face. The latter showed a sharp circular reflection peak at 40 Å, which was attributed to the diameter of the DNA–CTMA complex; an additional circular reflection peak observed from the side edge at about 4 Å was attributed to the distance between adjacent DNA strands. Yang et al.[13]

[*] Y. Ner, Prof. G. A. Sotzing
The Polymer Program, Department of Chemistry
University of Connecticut
97 N. Eagleville Rd., Storrs, CT 06269 (USA)
Fax: (+1) 860-486-4745
E-mail: sotzing@mail.ims.uconn.edu
Dr. J. G. Grote
US Air Force Research Laboratory, Wright-Patterson Air Force Base (USA)
Dr. J. A. Stuart
Institute of Materials Science
University of Connecticut
97 N. Eagleville Rd., Storrs, CT 06269 (USA)

[**] We thank N. Ogata for the generous donation of salmon DNA samples. G.A.S. gratefully acknowledges financial support by the National Science Foundation (DMR 0502928). We thank C. Norris and J. Gromek (University of Connecticut, Storrs) for their help during fluorescence microscopy and WAXD experiments, respectively.

Supporting information for this article is available on the WWW under http://dx.doi.org/10.1002/anie.200900885.

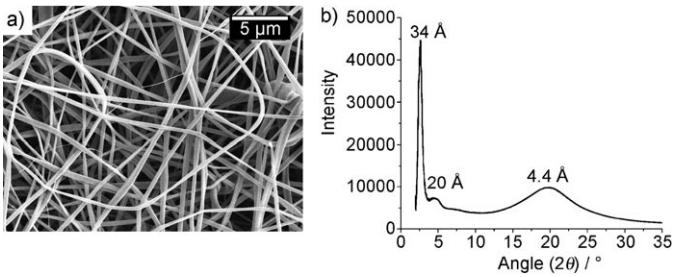

Figure 1. a) FESEM image and b) WAXD pattern of a self-standing electrospun DNA–CTMA nanofiber mesh produced from a 10% (w/w) solution of DNA–CTMA in ethanol/chloroform (3:1 w/w).

demonstrated that in stretched films of DNA–CTMA, the small-angle X-ray reflection at 41 Å changes from circular to a sharp spot because of alignment of the DNA in the stretching direction. However, upon drying the sample, this peak was observed at 36 Å. Figure 1b shows the wide-angle X-ray diffraction (WAXD) pattern of a dried DNA–CTMA self-standing nanofiber mesh. Circular reflection peaks at 34 and 4.4 Å are observed. The electrospun fibers in the nonwoven mesh adopt a completely random orientation with respect to each other. Hence, both circular reflection peaks described above are observed.[7] The distance between DNA strands is 34 Å, a value smaller than previously reported, which implies a more compact arrangement of DNA and CTMA phases in the nanofibers.

The complex, regular arrangement of the DNA and CTMA phases presents ample opportunities for association of small molecules and/or chromophores in discrete, isolated sites, including intercalation and/or groove binding with DNA, and entrapment within the CTMA surfactant phase. As such, careful selection of fluorophores will result in segregated populations isolated to different lattice locations. For the study presented herein, the fluorophores chosen were Cm102 and Hemi22 as donor and acceptor, respectively. This donor–acceptor pair produces a large Stokes shift, thereby providing excellent resolution of both donor and acceptor emission. Furthermore, these dyes are expected to interact with DNA through different mechanisms. Hemi22 has a very similar structure to that of (dimethylaminostyryl)-1-methylpyridinium iodide, which has been reported as a DNA minor-groove binding dye.[14] It has been demonstrated previously that upon association with DNA–CTMA, achiral Hemi22 orients along the chiral DNA double helices.[7] On the other hand, studies on the interaction between DNA and Cm102 support incorporation of the dye within the interior of the DNA helix (intercalation) while maintaining the native DNA structure.[15] Another dye molecule from the coumarin family, Coumarin 2, has also been reported to intercalate within the DNA double helix.[16]

The most likely spatial arrangement of dye molecules within the DNA–CTMA complex would be association of the acceptor dye's polar/cationic pyridinium-based head group in the DNA minor groove, with the donor dye intercalating between base pairs. Such an arrangement can reduce self-quenching, while simultaneously providing the necessary Förster donor–acceptor separation distance (the Förster radius is 1–10 nm for most dye pairs[17]). The doubly shaded region in Figure 2a and b shows spectral overlap in the emission spectra of the donor and absorption spectra of the acceptor in DNA–CTMA and poly(methyl methacrylate) (PMMA) spin-coated films, respectively. A significant red shift in the emission spectrum of both dyes is observed in the DNA–CTMA matrix, as compared to PMMA,[18] which indicates a highly polar and protic microenvironment around the dye molecules. Although the DNA–CTMA matrix is stoichiometrically charge neutral, the interior of the DNA double helix is polar,[15,19] which further supports association of both dyes with the DNA phase.

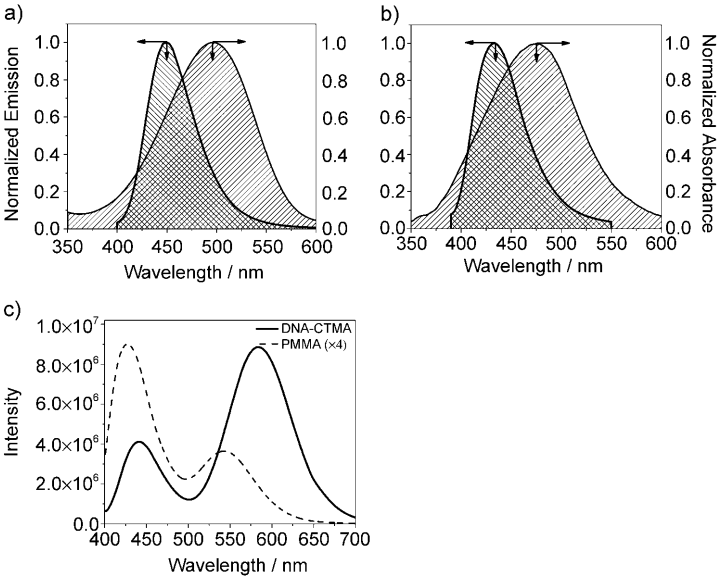

Figure 2. a) Normalized photoluminescence spectrum of DNA–CTMA films containing Cm102 (donor dye, $\lambda_{max}=450$ nm, $\lambda_{ex}=388$ nm) and the UV/Vis absorption spectrum of DNA–CTMA films containing the Hemi22 acceptor dye ($\lambda_{max}=496$ nm). b) Corresponding spectra of the same dyes in PMMA films (for donor dye $\lambda_{max}=430$ nm, $\lambda_{ex}=380$ nm and for acceptor dye $\lambda_{max}=474$ nm). c) Steady-state photoluminescence spectra for films of PMMA and DNA–CTMA with acceptor-to-donor molar ratio 1:5.

Figure 2c compares the photoluminescence spectra of multiple-dye-doped films of PMMA and DNA–CTMA. Although both matrices contained equal amounts of dyes, in the case of DNA more energy is transferred from donor to acceptor. In both matrices, donor emission provides excellent overlap with acceptor absorption, and thus the difference between energy-transfer efficiencies can be attributed to the well-defined organization of dyes by association within DNA, which not only promotes the energy transfer but also reduces self-quenching resulting from aggregation. (Note that the PMMA spectrum is presented as fourfold enlarged.)

Encapsulation of dyes to produce fluorescent nanofibers may enable a number of new technologies; dye-doped nanofibers have been utilized as nanometric light sources,[20]

as subwavelength optical waveguides,[21] and also in solar cells.[22] Electrochromic devices made from nanofibers showed 20-fold faster switching speeds than the analogous films.[23] Enhanced fluorescence in DNA–CTMA nanofibers[12] further strengthens such efforts. To study the effectiveness of the DNA–CTMA nanofiber matrix for energy transfer, the acceptor-to-donor molar ratio was varied systematically between 1:200 and 1:5. In all cases, the concentration of donor dye to DNA–CTMA was kept at 1.17% (w/w). At this concentration of dye, self-quenching as a result of aggregation is minimized.[10,24] Note that DNA–CTMA loaded with up to 25% (w/w) sulforhodamine fluorophore, equivalent to one dye molecule per two base pairs, showed no significant change in the DNA chirality.[24] Fluorescence microscopy images of donor-doped and 1:5 acceptor–donor-doped electrospun fibers are shown in Figure 3a and b, respectively. The fluorescence microscopy images clearly indicate the incorporation of the dye within the nanofibers.

Figure 3c shows the quenching behavior of the donor (Cm102) in the presence of the acceptor (Hemi22) through steady-state fluorescence measurements. With an increase in acceptor concentration, the magnitude of quenching at the donor emission maximum ($\approx$450 nm) increases and is accompanied by a significant increase in the acceptor emission intensity at $\approx$593 nm. Even at low acceptor concentrations (1 mole per 200 moles of donor), the influence of the acceptor emission maximum is distinguishable, which suggests efficient FRET between donor and acceptor dyes within the DNA–CTMA nanofibers. The effectiveness of energy transfer is further confirmed by comparing the nanofiber fluorescence emission at a doping ratio of 1:5 with that for nanofibers containing only acceptor (sample 1:0 in Figure 3c). For nanofibers with acceptor only, no significant fluorescence is observed, whereas nanofibers with an acceptor-to-donor ratio of 1:5 show a distinct peak corresponding to the acceptor emission maximum. The concentration of acceptor molecules was identical for both samples. As shown in Figure 3d, the FRET efficiency improves with increasing acceptor loading. Incomplete spectral overlap between the donor emission and acceptor absorption bands, and the suboptimal relative orientation of the emission and absorption dipoles of the donor and acceptor dyes, respectively, can limit the overall FRET efficiency. Despite these restrictions, however, the Cm102–Hemi22 pair displays substantial energy transfer in DNA–CTMA nanofibers, even at low acceptor loading.

Figure 4a shows a map for the emission of DNA–CTMA–Cm102–Hemi22 nanofibers with varying acceptor-to-donor ratios on a two-dimensional projection of the CIE (Commission Internationale de l'Eclairage) *xy* chromaticity diagram; with increasing acceptor concentration, the color changes from blue to orange, and passes through pure white. The sample with acceptor-to-donor molar ratio 1:20 is perceived as pure white-light emission with color coordinates (0.35, 0.34), which are very close to the exact white point (0.33, 0.33). The color temperature at this point was noted as 4650 K.

Figure 4b shows a digital photograph of DNA–CTMA–Hemi22–Cm102 nanofibers as a nonwoven mesh illuminated with UV light (see the Supporting Information). The last two samples in the bottom row contain the same amount of acceptor dye (Hemi22); however, in the right-hand sample no significant light emission was observed because of the absence of donor molecules and thus the absence of energy transfer. The conversion of UV light into white light in the nanofibers is also demonstrated by coating white-light-emitting DNA-based nanofibers onto 400-nm-emitting solid-state LEDs (Figure 4c). The implication of FRET-based simultaneous emission to generate visible light is that the emission color can be easily tuned not only by varying the acceptor-to-donor ratio, but also by changing the population density of the

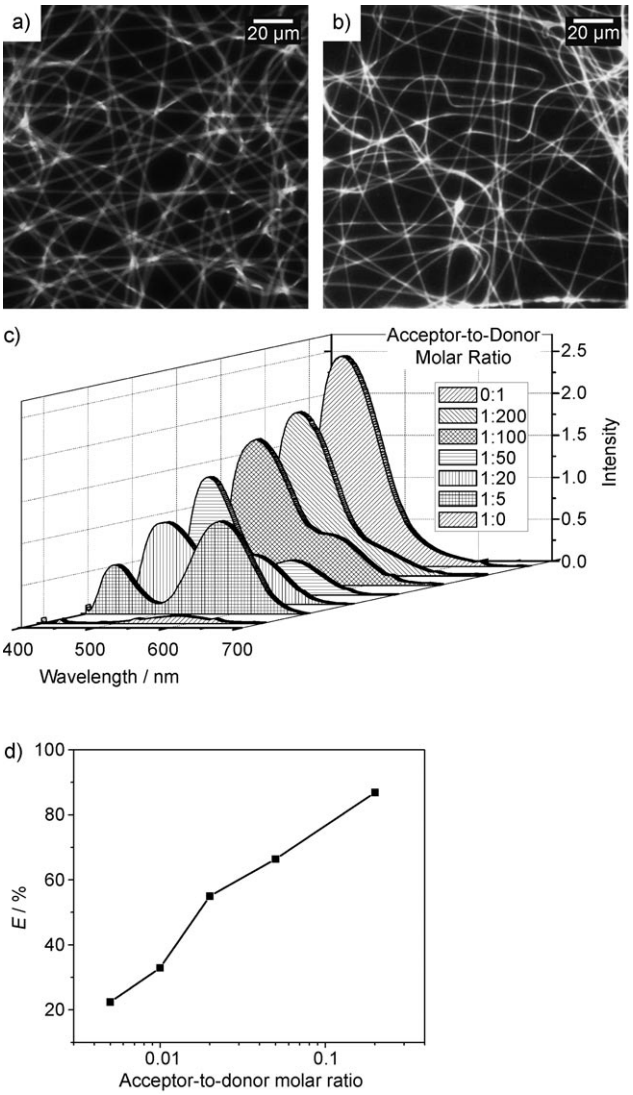

Figure 3. Fluorescence microscopy images of a) electrospun nanofibers of DNA–CTMA–Cm102 (donor) and b) DNA–CTMA–Cm102–Hemi22 with acceptor-to-donor ratio 1:5. c) Quenching curves of multiple-dye-doped DNA–CTMA nanofibers with increase in acceptor concentration (λ_{ex} = 388 nm). In all cases, the Cm102 donor concentration is 1.17% (w/w) relative to DNA. From left to right, the molar ratio of acceptor and donor varied from 1:5 to 1:200. The concentration of Hemi22 acceptor in the 1:5 sample and in the acceptor-only sample (1:0) is identical. d) FRET efficiency plotted against acceptor-to-donor molar ratio.

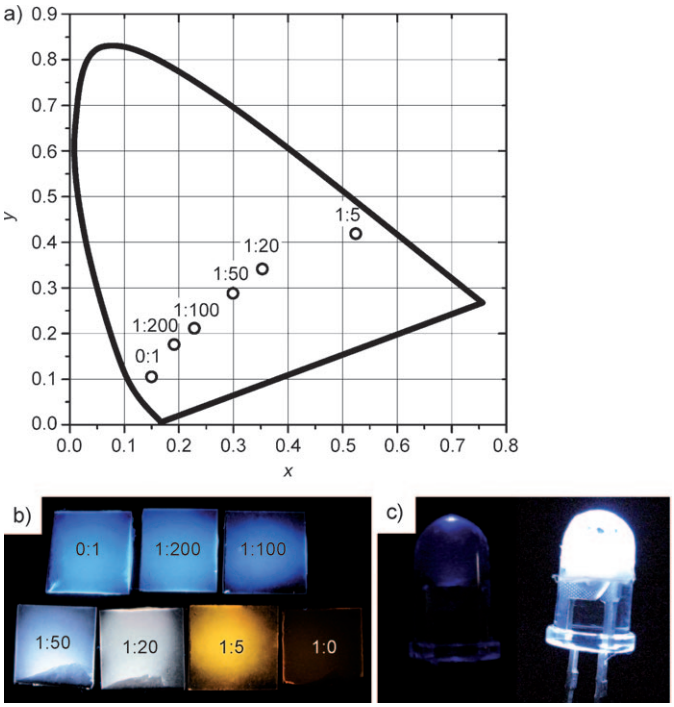

Figure 4. a) Chromaticity parameters of dye-doped DNA–CTMA nanofibers (circles) illuminated with UV light ($\lambda_{ex} = 365$ nm). For sample labeling, see Figure 3. b) Digital photograph of luminescent nanofiber meshes deposited on glass and illuminated at 365 nm with a UV lamp. The acceptor-to-donor molar ratios are indicated. c) 400-nm UV LEDs without (left) and with white-light-emitting DNA nanofiber coating (right).

acceptor and donor molecules in the matrix. By changing the total dye loading from 1.33 to 10% in the DNA matrix, the color temperature was tuned from cool white to warm white (see the Supporting Information).

In summary, we have demonstrated that solid-state DNA-based nanofibers can be an efficient matrix for FRET. The highly structured mesophasic morphology intrinsic to DNA–CTMA can sequester small molecules in a variety of specific nanoenvironments within the same matrix. Such an arrangement can isolate populations of donor and acceptor dyes from one another within the same matrix, thereby allowing higher loading levels without self-fluorescence quenching. Furthermore, as demonstrated by Li et al.,[25] electrospinning can be used to distribute fluorophores homogeneously in fibers to minimize interaction. As a matrix, DNA has proven to be an efficient optoelectronic material, and results from the present study will serve to strengthen such efforts. The possibility of an all-organic, non-phosphor-based white-light technology is appealing from the perspective of both environmental disposal and utilization of a renewable resource. In-house experiments have demonstrated the possibility of achieving a wide variety of colors—nearly the entire visible spectrum—through FRET-mediated conversion of UV light in multiple donor–acceptor systems; consequentially, light-harvesting antenna systems can be imagined. A variety of chemical sensor architectures are also conceivable, which simultaneously exploit the properties of DNA, nanofibers, and embedded fluorophores. For example, the higher surface area inherent to nanofibers might be utilized effectively to design sensors wherein the medium affecting the luminescence characteristics of either the fluorophore or DNA structure can be detected with dual signals. Our efforts are currently directed toward the design of novel optoelectronic and photonic architectures based upon these dye-impregnated DNA fibers.

Experimental Section

The DNA–cationic surfactant complex was prepared from salmon DNA (500 kDa). Briefly, an aqueous solution of DNA (1%, w/w) was prepared and a stoichiometric amount of an aqueous solution of CTMA (1%, w/w) was added over 4 h. The resultant precipitate was washed with water and dried overnight in a vacuum oven at 60 °C.[7,10] Cm102 and Hemi22 dyes were purchased from Exciton Inc. and Sigma–Aldrich, respectively.

Electrospinning was carried out with the spin dope consisting of DNA–CTMA (10%, w/w) in ethanol/chloroform (3:1, w/w). A homogeneous solution was obtained by heating at 60 °C for 30 min with constant stirring. Prior to electrospinning, the solution was stirred for another 5 min at room temperature. For dye doping, solutions of both dyes were prepared prior to addition to DNA–CTMA; for consistency, the sequence of addition was kept as Cm102 in ethanol followed by Hemi22 in chloroform. Electrospinning was performed at a potential of 20 kV and the distance between the electrodes was maintained at 17 cm. The rate of spinning was held at 0.8 mL h^{-1} by using a motorized syringe pump. A stable jet between the syringe needle assembly and the collector was obtained under these conditions. Fibers were collected on the ground electrode, which consisted of glass slides placed above a grounded copper plate. All experiments were carried out at ambient temperature and various fiber mat thicknesses were obtained by adjusting the time of spinning.

Films of DNA–CTMA and PMMA were obtained by spin-coating a solution (2%, w/w) of the respective polymer at 2500 rpm on glass slides. The DNA–CTMA solution was prepared in an analogous manner to that of preparing the electrospinning solution. However, in the case of PMMA, chloroform was used as the solvent.

Electron microscopic analysis was performed using a JEOL 6335F FESEM instrument. Fluorescence microscopy studies were performed with a Zeiss Axiovert 200M fluorescence microscope at an excitation wavelength of 365 nm and an emission window of 400–700 nm. Steady-state fluorescence measurements were performed on a Fluorolog-3 spectrofluorometer. Colorimetric measurements were performed with a PR-670 SpectraScan colorimeter (Photo Research, Inc., CA) under a laboratory UV lamp ($\lambda = 365$ nm). WAXD experiments were performed on an Xcalibur PX Ultra diffractometer (Oxford Diffraction) with a sample to Onyx CCD detector distance of 65 mm using $Cu_{K\alpha}$ radiation (wavelength $\lambda = 0.154$ nm). Before X-ray analysis, the fiber meshes were dried at 50 °C for 2 h in a laboratory vacuum oven.

The effectiveness of energy transfer was calculated by measuring the FRET efficiencies and using Equation (1), where I_{DA} and I_D are the donor fluorescence intensities in the presence and absence of the acceptor molecules, respectively.[17]

$$\%E = \left(1 - \frac{I_{DA}}{I_D}\right) \times 100 \quad (1)$$

Received: February 13, 2009
Published online: June 9, 2009

Keywords: DNA · electrospinning · energy transfer · nanostructures · self-assembly

[1] a) M. Berggren, A. Dodabalapur, R. E. Slusher, Z. Bao, *Nature* **1997**, *389*, 466 – 469; b) I. L. Medintz, A. R. Clapp, J. S. Melinger, J. R. Deschamps, H. Mattoussi, *Adv. Mater.* **2005**, *17*, 2450 – 2455.

[2] L. Wang, W. Tan, *Nano Lett.* **2006**, *6*, 84 – 88.

[3] T. Q. Nguyen, J. Wu, V. Doan, B. J. Schwartz, S. H. Tolbert, *Science* **2000**, *288*, 652 – 656.

[4] S. I. Yoo, S. J. An, G. H. Choi, K. S. Kim, G. C. Yi, W. C. Zin, J. C. Jung, B. H. Sohn, *Adv. Mater.* **2007**, *19*, 1594 – 1596.

[5] A. Adronov, S. L. Gilat, J. M. J. Fréchet, K. Ohta, F. V. R. Neuwahl, G. R. Fleming, *J. Am. Chem. Soc.* **2000**, *122*, 1175 – 1185.

[6] A. Del Guerzo, A. G. L. Olive, J. Reichwagen, H. Hopf, J. P. Desvergne, *J. Am. Chem. Soc.* **2005**, *127*, 17984 – 17985.

[7] L. Wang, J. Yoshida, N. Ogata, S. Sasaki, T. Kajiyama, *Chem. Mater.* **2001**, *13*, 1273 – 1281.

[8] K. Tanaka, Y. Okahata, *J. Am. Chem. Soc.* **1996**, *118*, 10679 – 10683.

[9] A. J. Steckl, *Nat. Photonics* **2007**, *1*, 3 – 5.

[10] J. G. Grote, J. A. Hagen, J. S. Zetts, R. L. Nelson, D. E. Diggs, M. O. Stone, P. P. Yaney, E. Heckman, C. Zhang, W. H. Steier, A. K. Y. Jen, L. R. Dalton, N. Ogata, M. J. Curley, S. J. Clarson, F. K. Hopkins, *J. Phys. Chem. B* **2004**, *108*, 8584 – 8591.

[11] Y. Kawabe, L. Wang, S. Horinouchi, N. Ogata, *Adv. Mater.* **2000**, *12*, 1281 – 1283.

[12] Y. Ner, J. G. Grote, J. A. Stuart, G. A. Sotzing, *Soft Matter* **2008**, *4*, 1448 – 1453.

[13] C. Yang, D. Moses, A. J. Heeger, *Adv. Mater.* **2003**, *15*, 1364 – 1367.

[14] C. V. Kumar, R. S. Turner, E. H. Asuncion, *J. Photochem. Photobiol. A* **1993**, *74*, 231 – 238.

[15] R. S. Coleman, M. A. Berg, C. J. Murphy, *Tetrahedron* **2007**, *63*, 3450 – 3456.

[16] A. Bodi, K. E. Borbas, J. I. Bruce, *Dalton Trans.* **2007**, 4352 – 4358.

[17] S. S. Vogel, C. Thaler, S. V. Koushik, *Science's STKE* **2006**, *331*, re2.

[18] The emission maxima for Cm102 in PMMA and DNA–CTMA were 430 and 450 nm, respectively, at equivalent dye concentrations. Hemi22 behaved similarly, with emission maxima of 560 nm in PMMA and 593 nm in DNA–CTMA.

[19] E. B. Brauns, C. J. Murphy, M. A. Berg, *J. Am. Chem. Soc.* **1998**, *120*, 2449 – 2456.

[20] J. M. Moran-Mirabal, J. D. Slinker, J. A. Defranco, S. S. Verbridge, R. Ilic, S. Flores-Torres, H. Abruna, G. G. Malliaras, H. G. Craighead, *Nano Lett.* **2007**, *7*, 458 – 463.

[21] a) H. Liu, J. B. Edel, L. M. Bellan, H. G. Craighead, *Small* **2006**, *2*, 495 – 499; b) I. Cucchi, F. Spano, U. Giovanella, M. Catellani, A. Varesano, G. Calzaferri, C. Botta, *Small* **2007**, *3*, 305 – 309.

[22] K. Onozuka, B. Ding, Y. Tsuge, T. Naka, M. Yamazaki, S. Sugi, S. Ohno, M. Yoshikawa, S. Shiratori, *Nanotechnology* **2006**, *17*, 1026 – 1031.

[23] S. Y. Jang, V. Seshadri, M. S. Khil, A. Kumar, M. Marquez, P. T. Mather, G. A. Sotzing, *Adv. Mater.* **2005**, *17*, 2177 – 2180.

[24] A. J. Steckl, H. Spaeth, K. Singh, J. Grote, R. Naik, *Appl. Phys. Lett.* **2008**, *93*, 193903.

[25] M. Li, J. Zhang, H. Zhang, Y. Liu, C. Wang, X. Xu, Y. Tang, B. Yang, *Adv. Funct. Mater.* **2007**, *17*, 3650 – 3656.

